Qiong Zhang · Haijun Yang · Yafang Zhong
Dongxiao Wang

An idealized study of the impact of extratropical climate change on El Niño–Southern Oscillation

Abstract Extratropical impacts on the tropical El Niño–Southern Oscillation (ENSO) are studied in a coupled climate model. Idealized experiments show that the remote impact of the extratropics on the equatorial thermocline through oceanic tunnel can substantially modulate the ENSO in both magnitude and frequency. First of all, an extratropical warming can be conveyed to the equator by the mean subduction current, resulting in a warming of the equatorial thermocline. Second, the extratropical warming can weaken the Hadley cells, which in turn slow down the mean shallow meridional overturning circulations in the upper Pacific, reducing the equatorward cold water supply and the equatorial upwelling. These oceanic dynamic processes would weaken the stratification of the equatorial thermocline and retard a buildup (purge) of excess heat content along the equator, and finally result in a weaker and longer ENSO cycle. This study highlights a nonlocal mechanism in which ENSO behavior is related to the extratropical climate conditions.

Q. Zhang
LASG, Institute of Atmospheric Science,
Chinese Academy of Sciences, Beijing, China

H. Yang (✉)
Department of Atmospheric Science and Laboratory for Severe
Storm and Flood Disasters, School of Physics,
Peking University, 209 Chengfu Road,
100871 Beijing, China
E-mail: hjyang@pku.edu.cn
Tel.: +86-10-6275-7436
Fax: +86-10-6275-1094

Y. Zhong
Center for Climatic Research and
Department of Atmospheric and Oceanic Sciences,
University of Wisconsin–Madison, Madison, WI, USA

D. Wang
Laboratory of Tropical Marine Environmental Dynamics,
South China Sea Institute of Oceanology,
Chinese Academy of Sciences, Guangzhou, China

1 Introduction

It has been established that the tropical El Niño–Southern Oscillation (ENSO) has a significant impact on the global climate through atmospheric teleconnections (e.g., Lau 1997; Alexander et al. 2002). Observational and modeling studies have demonstrated a clear link between sea surface temperature (SST) anomalies in the equatorial Pacific with those in the North Pacific (Zhang and Wallace 1996; Lau 1997; Zhang et al. 1998a), north tropical Atlantic (Enfield and Mayer 1997; Wang 2002), North Atlantic (Hoerling et al. 2001; Lu et al. 2004) and Indian Oceans (Yu and Rienecker 1999). However, the ENSO itself may be subject to change due to an overall background change in the global climate (Fedorov and Philander 2000), or (and) a remote impact of the extratropics (Gu and Philander 1997) or (and) just the local nonlinearities within the tropical atmosphere–ocean system (Timmermann and Jin 2002).

Paleoclimatic studies reveal that ENSO has undergone significant climate shifts in the history in response to a background climate change (Liu et al. 2000; Cole 2001; Tudhope et al. 2001; Rosenthal and Broccoli 2004). It has also changed during the past two decades (Fedorov and Philander 2000). These findings have led to speculations that ENSO may be subject to change in the future as a result of global warming. However, uncertainties and disputes about ENSO behavior in a warming climate exist for different models (Collins 2000a). Forced by a future greenhouse warming, ENSO amplitude could be increased due to a stronger equatorial thermocline (Timmermann et al. 1999; Collins 2000b), or decreased due to a reduced time-mean zonal SST gradient (Knutson et al. 1997), or even unchanged because of a negligible changes in mean temperature and

zonal SST gradient in the equatorial Pacific (Meehl et al. 1993; Tett 1995). ENSO frequency also could be increased due to the increase in meridional temperature gradients (Collins 2000b) or unchanged (Knutson et al. 1997). The ENSO behavior appears to depend strongly on the mean climate that is related to model responses to the model physics, resolution and sub-scale processes (Collins 2000a).

The tropical climate can be affected by the extratropics through both the atmospheric bridge (AB) of Hadley cells and oceanic tunnel (OT) of meridional overturning circulations (Gu and Philander 1997; Wang and Weisberg 1998; Barnett et al. 1999; Kleeman et al. 1999; Weaver 1999; Pierce et al. 2000), which could eventually determine the stability of tropical coupled ocean–atmosphere modes. Therefore, although ENSO primarily originates in the tropics, the remote impact of the extratropics must be taken into account when we study ENSO behavior in a global change framework. Furthermore, because oceanic processes are deeply involved in the extratropical-induced tropical mean climate change, which nearly account for one-third of the SST change and 80% of the subsurface temperature change in the equator as indicated in the recent works of Liu and Yang (2003) and Yang and Liu (2005), the oceanic dynamics play an important role in altering the ENSO properties.

This study focuses on the extratropical modulation of ENSO. Despite the numerous researches on the ENSO behavior in the tropical–extratropical interactions and in a global warming climate, it is still unclear how much the ENSO would change in response to a given extratropical forcing, and what the relative roles of the AB and OT would play in the ENSO change. These questions are explored in this paper by employing a unified fully coupled climate model. With the help of idealized extratropical warming experiments, we quantitatively assessed the extratropical modulations of ENSO. It is shown that the remote impact of the extratropics on the equatorial thermocline through OT can substantially modulate the ENSO in both magnitude and frequency, because of the dominant role of the OT in conveying the extratropical anomaly to the equator. A weaker and longer ENSO cycle is likely in a climate forced by an extratropical warming, because the ocean dynamic adjustment would result in a weakening of the stratification of the equatorial thermocline and a retarding of a buildup (purge) of excess heat content along the equator. This study highlights the nonlocal mechanism in which ENSO behavior may be related to the extratropical climate conditions. This work can be also understood as a study of ENSO sensitivity to an idealized global warming where the maximum SST increase occurs in the high latitudes.

This paper is organized as follows. Section 2 introduces the coupled model and experiments. Section 3 briefly describes the tropical mean climate change in response to an extratropical warming. Section 4 anatomizes the changes in ENSO properties in response to the background climate change as well as the relative roles of the AB and OT. Conclusions and discussions are provided in Section 5.

2 Model and approach

The model used here is the Fast Ocean–Atmosphere Model (FOAM) developed jointly at University of Wisconsin–Madison and the Argonne National Laboratory (Jacob 1997). The Atmospheric model is a parallel version of the National Center for Atmospheric Research (NCAR) Community Climate Model version 3 (CCM3). The ocean model was developed following the Geophysical Fluid Dynamics Laboratory (GFDL) Modular Ocean Model (MOM). The FOAM used here has an atmospheric resolution of R15 and an oceanic resolution of $1.4°$ latitude$\times 2.8°$ longitude$\times 32$ vertical levels. Without flux adjustment, the fully coupled control simulation (CTRL) has been integrated for over 1,000 years, showing no apparent climate drifts. FOAM has been used successfully in the study of ENSO (Liu et al. 2000), Atlantic climate variability (Liu and Wu 2000) and Pacific decadal variability (Liu et al. 2002; Wu et al. 2003). For example, the simulated ENSO has a realistic period of 2–5 years and amplitude of about 75% of the observations (Liu et al. 2000). The leading EOF of decadal low-passed SST exhibits an ENSO-like pattern that also correlates well with observations (Wu et al. 2003).

Mean climate changes in the extratropics can cause remarkable changes in the background climate of the tropical ENSO, through both the AB and OT (Liu and Yang 2003; Yang and Liu 2005), which eventually modulate the statistics of ENSO behavior. To identify the mean climate impact of the extratropics on ENSO, "partial coupling" (PC) technique is used in FOAM. Using this approach, full ocean–atmosphere coupling is allowed only in some selected region; elsewhere, the coupling is suppressed and the annual cycle of climatological SST from model CTRL is prescribed to force the model atmosphere or ocean. The PC provides a modeling technique for quantitatively assessing climate interactions between different geographic regions.

Three experiments are performed to study the sensitivity of ENSO to extratropical forcing. First, to assess the full impact of the extratropical warming on ENSO, a PC experiment ABOT (atmospheric bridge/ oceanic tunnel) is performed, in which a 2°C SST anomaly is "seen" by both the atmosphere and ocean in the global extratropics ($> |30°|$ latitude) and is then "carried" equatorward by both the AB and OT. Specifically, the ocean and atmosphere in ABOT remain fully coupled within the global tropics ($< |30°|$ latitude), but become only partially coupled in the extratropics. There, the atmosphere is forced by the heat flux that is calculated based on the prescribed SST seasonal cycle of the CTRL plus 2°C; the atmospheric variables are then used to calculate the fluxes of heat, freshwater and momentum at each time step to force

the ocean, but the prescribed SST is still given back to force the atmosphere. Second, to assess the individual role of ocean dynamics, an OT experiment is conducted. It is the same as ABOT except for a modified PC in the extratropics. There, the surface ocean is restored towards the prescribed SST seasonal cycle of CTRL plus 2°C, while the atmosphere is forced by the prescribed SST seasonal cycle of CTRL only. As such, only the ocean "sees" a 2°C SST warming and therefore contributes to the equatorward subduction of extratropical SST anomaly. Third, to assess the individual role of atmosphere dynamics, an AB experiment is conducted. It is same as ABOT except that the oceanic teleconnection tunnel is "blocked" by inserting a "sponge wall" at 27–33° latitude bands in which temperature and salinity are restored towards their seasonal climatology. Thus, the extratropical 2°C SST warming can affect the tropics only through the AB. Note that the 2°C SST forcing and the prescribed SST seasonal cycle are only applied to the regions without sea ice. There is still fully coupled between sea ice and atmosphere. All the experiments start from the 800th year of the CTRL run. ABOT and OT are integrated for 200 years, when the upper ocean has reached quasi-equilibrium. Since the tropical subsurface ocean in AB is hardly changed, AB is only integrated for 50 years when the atmosphere and the surface ocean have reached quasi-equilibrium.

For each PC experiment, a parallel PC control simulation is performed. All the mean climate changes are derived as the difference of each PC experiment and its respective control. Each PC control simulation is per-

formed to avoid the model drift that may arise due to the PC scheme. Therefore, each PC control has exactly the same configuration as the PC sensitivity experiment except in the PC region where no anomalous SST is added to the prescribed seasonal cycle of CTRL (e.g., the extratropical SST to the atmosphere is prescribed simply as the seasonal cycle of CTRL for ABOT control). These PC controls do not have significant drifts from the fully coupled CTRL, such that our major results do not change significantly regardless of using the PC control or the fully coupled CTRL as the base run to derive climate anomalies.

3 Changes in the tropical mean climate

Accomplished by both the AB and OT in ABOT, a 2°C extratropical SST warming can increase equatorial SST by about 0.9°C (Fig. 1). Based on experiments AB and OT, the individual contribution of the AB and OT is about 0.6 and 0.3°C, accounting for 70 and 30% of the total equatorial SST warming in ABOT, respectively. Experiment ABOT shows that after the onset of the extratropical warming, equatorial SST increases rapidly by more than 0.5°C in the first few years, and gradually reaches quasi-equilibrium after a 100 years (Fig. 1a). The quick extratropical impact through the atmospheric bridge is clearly shown in AB. In ABOT, a warming SST in the extratropics can force a tropical SST warming of about half its magnitude, representing a significant extratropical control on tropical climate.

Fig. 1 Evolution of anomalous annual mean (**a**) SST and (**b**) upper ocean temperature (40–400 m average) in ABOT (*solid black*), AB (*solid grey*) and OT (*dashed grey*). The temperature is averaged globally within 10° of the equator. The 21-year running mean is also plotted for each curve as the heavy lines. Two hundred years data for ABOT and OT and 50 years data for AB is plotted. The anomalous SST and subsurface temperature averaged in the last 100 years of ABOT and OT, and in the last 50 years of AB are labeled at the *right edge* of the figures. The anomaly in each experiment is relative to its own control run which has the identical settings as the respective PC experiments except for the absence of a 2°C SST anomaly on the prescribed seasonal cycle of CTRL
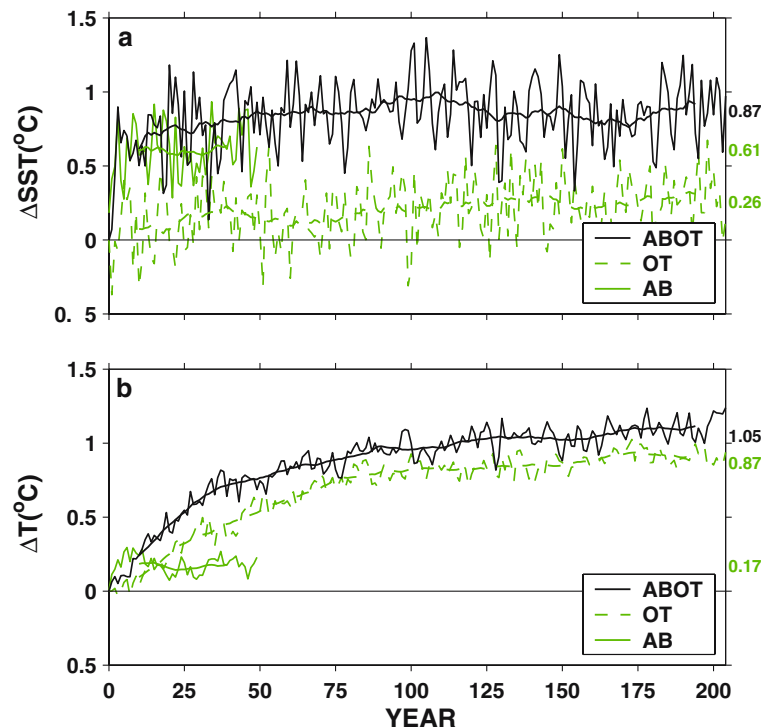
The OT, while only contributing a small portion of the equatorial temperature change on the surface, dominates the change in the subsurface temperature and determines the equatorial thermocline structure (Fig. 1b). Indeed, over 80% of the subsurface temperature change in ABOT is accounted for by equatorward oceanic subduction process in OT (Fig. 1b). The fast atmospheric bridge in AB is ineffective in changing equatorial temperature in the subsurface because the strong equatorial upwelling inhibits the downward penetration of the effect of the surface atmospheric forcing (Figs. 1b and 2c). In the equatorial upper ocean, the temperature anomaly is nearly uniform in the subsurface in ABOT (Fig. 2a), decreases upward towards the surface in OT (Fig. 2b), but decreases downward towards the subsurface in AB (Fig. 2c). This occurs because the SST is warmed from both sides of the surface in ABOT, but mainly from below by the ocean tunnel in OT, and from above by the atmosphere bridge in AB. In ABOT and OT, the overall vertical temperature gradient in the equatorial band is weakened due to the equatorward warm water subduction (Fig. 3a, b). This is particularly clear in OT (Fig. 3b) because there is

Fig. 3 Mean temperature changes in the upper equatorial Pacific averaged in a 5°N–5°S equatorial strip in year 150–200 for (a) ABOT, (b) OT and in year 1–50 for (c) AB. Contour intervals are 0.1°C. The *thick dashed* and *dotted lines* represent the depth of the 20°C isotherm for PC control and PC experiment, respectively
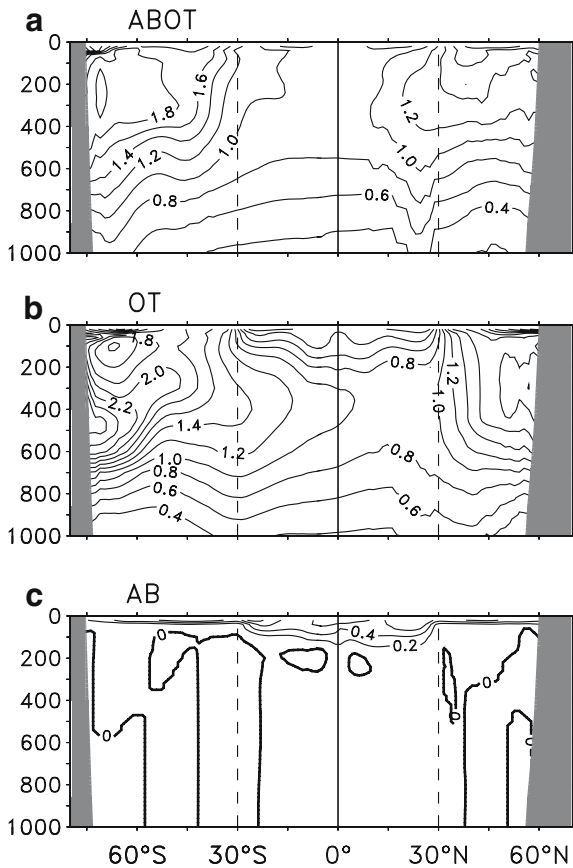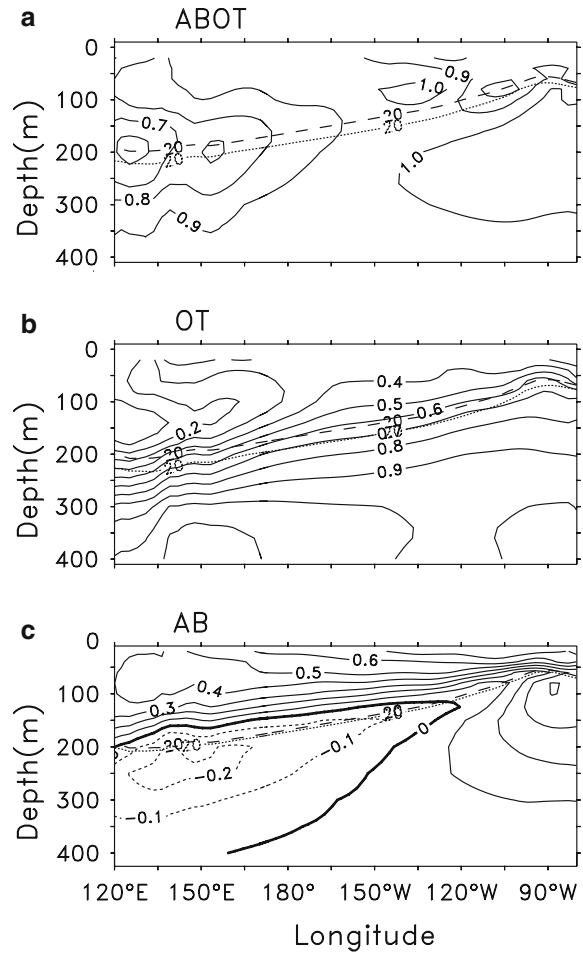
Fig. 2 Zonal mean temperature changes in the upper Pacific averaged in year 150–200 for (a) ABOT, (b) OT and in year 1–50 for (c) AB. Contour intervals are 0.2°C. The temperature change in each experiment is relative to its own control run

no anomalous forcing from the atmosphere. In ABOT (Fig. 3a), the subsurface water in the eastern Pacific warms more than the surface water, because weakening in mean equatorial trade wind tends to reduce the east–west tilt of the equatorial thermocline and thus suppress the cold water upwelling in the eastern equatorial Pacific. In AB (Fig. 3c), the vertical stratification along the equator is enhanced. But this is only confined in the upper thermocline above 200 m depth since the warming effect of the atmospheric forcing has very limited downward penetration.

The mean state changes in the tropics in response to the extratropical warming are consistent with the changes in the atmospheric Hadley cells and oceanic meridional overturning circulation. For example, in ABOT the Hadley cell is weakened because of the reduced meridional SST contrast. The oceanic meridional overturning circulation in ABOT is also slowed down in response to the weakened Hadley cell. One can find more details in Yang and Liu (2005).

4 ENSO variability

4.1 ENSO in CTRL run

The modeled ENSO in the control run has a reasonable spatial pattern and a realistic period of 2–5 years when compared with observations (Fig. 4). The first EOF mode of the tropical SST anomaly is the ENSO mode that accounts for 16% of the total SST variance (Fig. 4a). This ENSO mode has the maximum amplitude located in the western half of the equatorial Pacific, which is partly due to the over-westward spread of the equatorial cold tongue in the coupled model's control simulation. The power spectrum of the time series of the ENSO mode (Fig. 4b) shows two interannual peaks located at the 25th and 40th months, respectively. Both peaks pass the 90% confidence level.

4.2 ENSO response to extratropical warming

4.2.1 Change in ENSO amplitude

The statistics of the ENSO variability show extensive changes in amplitude, frequency and spatial pattern in response to the extratropical warming. Relative to the control simulation, the time evolution of the SST anomaly in Nino-3 region (150°W–90°W, 5°N–5°S) in ABOT experiment shows a reduced amplitude (Fig. 5). The mean standard deviation (SD) of the Nino-3 SST anomaly for the last 60 years is 0.44°C in ABOT control and 0.35°C in ABOT experiment, showing a 20% reduction in amplitude (Fig. 5b). This reduction passes the F-test of 95% significance level. Here the SST anomalies are obtained as follows: first, the mean seasonal cycle of each run is removed; second, the secular linear trend of each run is subtracted; third, a band-pass filter of 5–85 months is further applied. Therefore, the resultant SST variabilities only contain ENSO timescale information and have excluded both the monthly and decadal timescale information.

The amplitude of ENSO variability is not uniformly reduced in the tropics (Fig. 6). Relative to ABOT con-
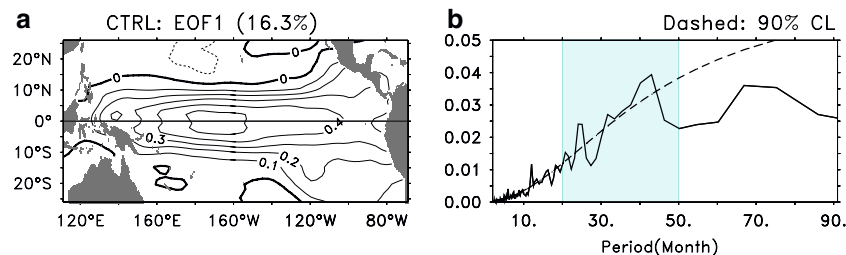

Fig. 5 Time series (**a**) and standard deviations (SD) (**b**) of the monthly SST anomalies averaged over Nino-3 region (150°W–90°W, 5°N–5°S) for ABOT control (*solid lines*) and experiment (*dashed lines*). In (**b**), a low-pass filter with a sliding window of 10-year wide is used to calculate the SD. The *straight lines* in (**b**) represent the mean SD over the first 50 years and the last 60 years

trol, the most remarkable SST variability change in ABOT experiment occurs in the cold tongue region of the central and eastern tropical Pacific with a decrease of more than 20%, while in the warm pool region of the western Pacific the average decrease is 5% which is narrowly confined to within 10° of the equator (Fig. 6a). Due to the strong coupling between the SST and the thermocline in the eastern Pacific (Zelle et al. 2004), the SD of the thermocline depth (represented by 20°C isotherm depth) in ABOT experiment is also decreased by more than 15% in the equatorial region, with the change most visible in the eastern Pacific (Fig. 6b).

Moreover, El Niño and La Niña, which consist of the positive and negative phases of an ENSO cycle, respectively, are not symmetrically affected by the extratropical warming (Fig. 7). Statistically, compared with the La Niña, the El Niño is less suppressed by the background warming in ABOT experiment. In the eastern Pacific, the amplitude of El Niño is reduced by 10% (Fig. 7c), while that of La Niña is reduced by nearly 30% (Fig. 7d). To investigate further the changes in the ENSO statistics,

Fig. 4 a The first EOF mode of the tropical SST anomaly within 25° of the equator in ABOT control and (**b**) the power spectrum of the time series of the first EOF mode. In (**b**), the 90% confidence level is plotted as the *dashed line*, and the *shadowed region* highlights an interannual band with the period between 2 and 5 years
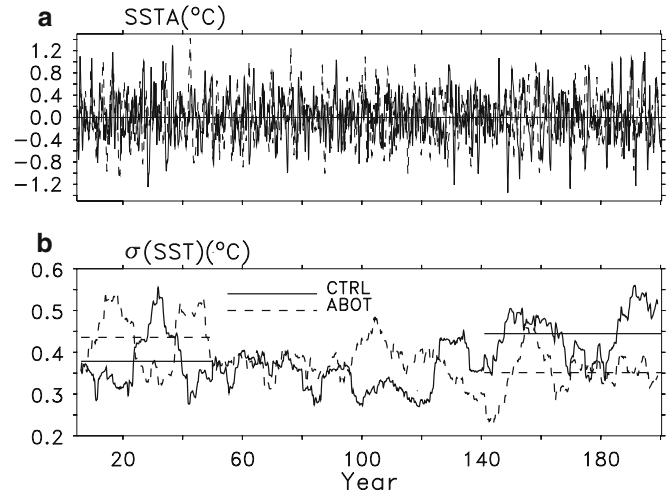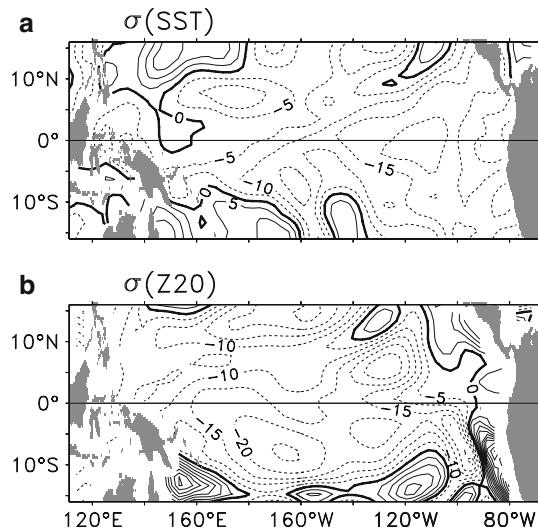
Fig. 6 Spatial patterns of the SD percentage changes in (**a**) the tropical SST and (**b**) the 20°C isotherm depth in ABOT experiment. The percentage change is calculated as the SD difference between ABOT experiment and control divided by that in ABOT control in the last 60 years (unit in %)

Fig. 8 The difference in the occurrence of warm and cold months between ABOT control and ABOT experiment. The *upper half* represents the warm month differences between ABOT control and ABOT experiment, while the *lower half* represents the cold month differences. From the *top* to *bottom* the *four shadowed boxes* represent the difference in the number of warm months with SST anomalies above 0.5°C and within 0–0.5°C, and cold months with SST anomalies within −0.5 to 0°C and below −0.5°C, respectively. The *shadowed boxes* in the *left half* represent the fewer occurrences of the warm (cold) months in ABOT experiment than that in ABOT control, while those in the *right half* represent the contrary

we calculate the frequency distributions of monthly SST anomalies for the last 60 years in ABOT. Figure 8 shows that both the extreme warm and cold months in ABOT experiment occur less than those in ABOT control. Furthermore, the occurrence of the strong cold months with SST anomaly lower than -0.5°C is decreased more than that of the strong warm months with SST anomaly higher than 0.5°C (33 vs 24). Figures 7 and 8 suggest a skewed effect of the extratropical warming on the ENSO cycle in ABOT.

The decrease in ENSO amplitude in the warmed climate of ABOT is due to the relaxation of the equatorial trade winds, the weakened vertical temperature stratification and the deepening in the equatorial thermocline (Figs. 2 and 3). These changes in background state play critical roles in determining the stability of the tropical ocean–atmosphere coupled modes (Fedorov and
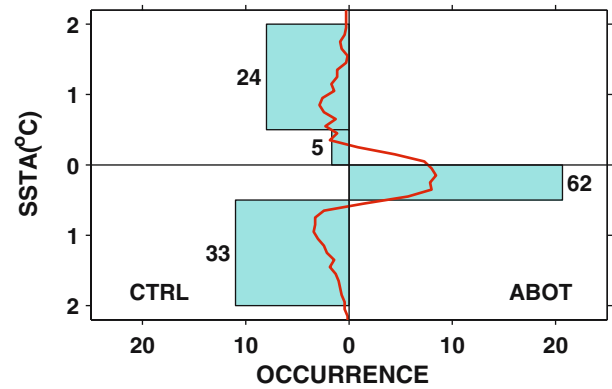
Philander 2001). The weakening in mean equatorial trade winds reduces the east–west tilt of the equatorial thermocline and thus suppresses the cold water upwelling in the eastern equatorial Pacific. Because of the subsurface warming in ABOT and OT, the equatorial thermocline is weakened, and the depth of the mean 20°C isotherm (dashed and dotted lines in Fig. 3a, b), a proxy of thermocline depth, is therefore moved downward by more than 20 m. All these changes tend to stabilize the natural modes of oscillation of the tropical coupled ocean–atmosphere system, and eventually damp the ENSO variability (Fedorov and Philander 2001; Timmermann 2001). Furthermore, the overall warming in the upper equatorial Pacific as well as the suppressed cold water upwelling cause the change in ENSO variability to be strongly skewed, with El Niño being less affected than La Niña.

Fig. 7 The composite (**a**) El Niño and (**b**) La Niña in ABOT control and the changes of (**c**) El Niño and (**d**) La Niña in ABOT experiment. The composite El Niño (La Niña) is obtained from the five largest warm (cold) events in the last 60 years. The El Niño (La Niña) change is calculated as the composite SST anomalies of the five largest warm (cool) events in ABOT experiment subtracted by those in ABOT control
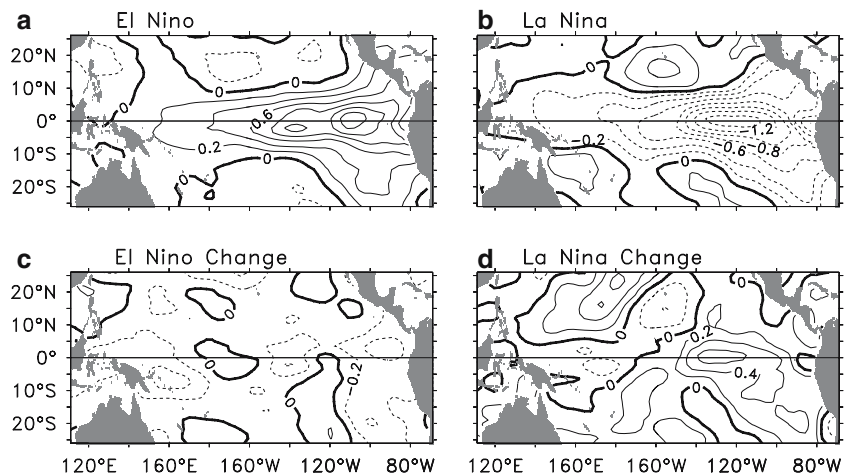
It is worth to emphasize that the OT is crucial to the modulation of the ENSO behavior. In ABOT experiment, the extratropical modulation of ENSO through the OT is accomplished by not only the slowdown of the mean shallow meridional overturning circulation, which would result in a less equatorward cold water transport and a weaker equatorial upwelling, but also the equatorward subduction of anomalous warm water by mean circulation. In OT experiment, only the warm anomalies subduction from the extratropics is responsible for the ENSO change because the mean overturning circulations here remain almost unchanged (Yang and Liu 2005). Despite the different mechanism in ABOT and OT experiments, it is these oceanic processes that increase the temperature and depth of the equatorial thermocline, weaken the vertical temperature gradient in the tropics and eventually reduce the ENSO amplitude.

The AB alone appears to play a role contrary to that of OT in the modulation of ENSO behavior. Figure 9 clearly shows an enhanced SST SD in AB experiment than in AB control. In AB, the remote impact of the extratropics on the tropical SST and subsurface temperature is accomplished only through the AB because of the blocking of the oceanic passage by the extratropical sponge walls. The vertical stratification of the thermocline along the equator is enhanced (Fig. 3c), which is similar to the scenario forced by a gradually increased CO_2 in Timmermann et al. (1999). In Fig. 9, we only plot the SST SD in the first 50 years because the atmospheric process acts rapidly so that the tropical air–sea system has reached the quasi-equilibrium. Figure 9a, b are same as Figs. 5b and 6a, respectively, but only for the first 50 years of AB. The Nino-3 SST SD is increased by nearly 15% in AB experiment (Fig. 9a). The most remarkable SST SD change (Fig. 9b) in AB occurs also in the cold tongue region which is similar to that in ABOT (Fig. 6a), but with an increase of about 10%. The enhanced ENSO amplitude can be also seen in the first 50 years simulation of ABOT (Fig. 5b) when the oceanic process has not yet fully taken effect (Yang and Liu 2005). This is consistent with the argument that the interannual variability may be increased because of a more energetic air–sea interaction in a warming climate caused by a gradually increased CO_2 (e.g., Timmermann et al. 1999).

In summary, because the OT and the AB act on different time scales—the oceanic process occurs on interannual to decadal time scales while the atmospheric adjustment occurs on monthly time scale, the ENSO would respond to the extratropical forcing differently at different time stages. In a quasi-equilibrium coupled system, the oceanic processes would reverse the effect of the AB, and ultimately determine the stability of the tropical coupled system, because the OT dominates more than 80% of the tropical thermocline temperature change (Liu and Yang 2003; Yang and Liu 2005).
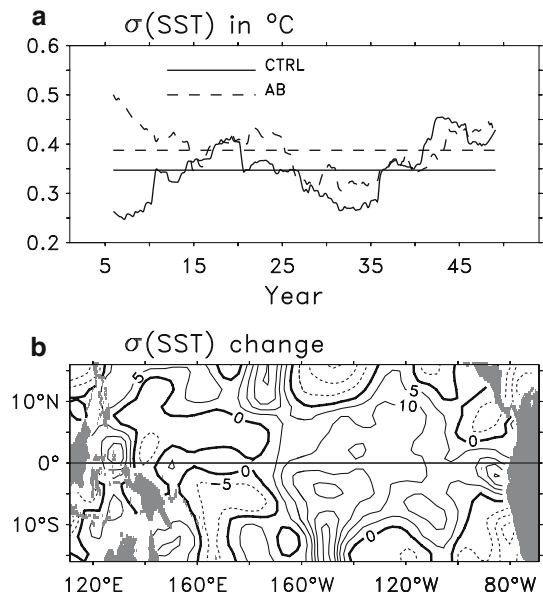

Fig. 9 Same as Figs. 5b and 6a, but for AB control and AB experiment in the first 50 years

4.2.2 Change in ENSO frequency

The remote modulation of the extratropical warming could also lengthen the ENSO period. Figure 10b shows that the power spectrum of Nino-3 SST anomaly has the primary peak located at the 40th month for ABOT control (solid line) and the 50th month for ABOT experiment (dashed line), respectively. Both peaks are well above the 95% confidence level (long dashed line).
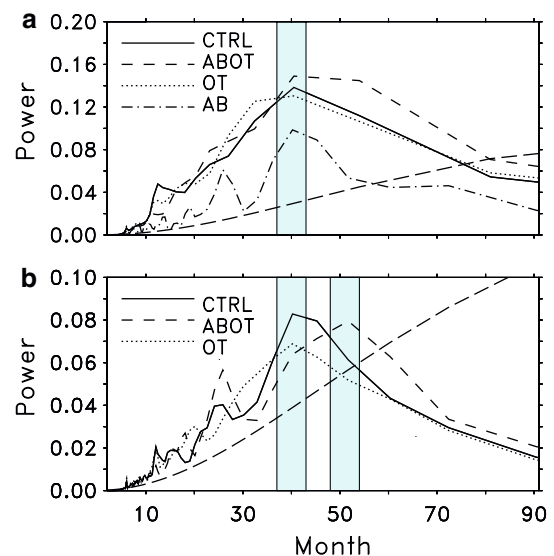

Fig. 10 Power spectra of Nino-3 SST anomalies for ABOT control (*solid line*), ABOT experiment (*dashed line*), OT experiment (*dotted line*) and AB experiment (*dotted–dashed line*) in (**a**) the first 20 years and (**b**) the last 60 years of the integrations. The 95% confidence level is plotted as the *long-dashed line*. The *shadowed regions* highlight the primary peaks located at nearly 40th and 50th months

This suggests a shift to longer period of the ENSO in the warmed climate of ABOT experiment. However, the power spectrum of the Nino-3 SST anomaly in OT experiment does not show any shift in ENSO period, in which the primary peak is still located at the 40th month (dotted line). (The power spectra of Nino-3 SST for ABOT control and OT control are very similar, so that here we choose the former as the reference for comparison.) Note that although only the data in the last 60 years are used to calculate the power spectra in Fig. 10b, the frequency shift in ABOT experiment is statistically robust because it is also present in an arbitrary period of the time series that excludes the first 20–30 years, as well as in the raw data sets that have no filtering applied. It is also robust that the ENSO frequency in OT experiment remains unchanged.

The shift of ENSO frequency in ABOT experiment can be attributed to the slowdown of the mean wind-driven meridional overturning circulation in the upper Pacific. It has been mentioned before that the mean shallow meridional overturning circulation in ABOT experiment is slowed down due to a weakening of the Hadley circulation caused by the extratropical warming. Figure 11a shows that the annual mean meridional overturning circulation in ABOT experiment is weakened by more than 10%. In particular, the shallow tight equatorial cells within about 5° of the equator in the upper 200 m in both hemispheres are reduced significantly. The meridional overturning circulation plays a very important role in the interaction between the subtropical and equatorial oceans (Liu et al. 1994; McCreary and Lu 1994). Figure 11b shows that the subtropical water subducts in the region of downward Ekman pumping (around 30°N/S) and flows equatorward at

depth, rises to the surface at the equator and returns poleward by means of Ekman drift. Therefore, the slowdown of the meridional overturning circulation could result in a change in the equatorial warm water volume (WWV) which is responsible for the ENSO occurrences.

The WWV, defined as the water above 20°C isotherm over the region 5°S–5°N, 120°E–80°W (Meinen and McPhaden 2000), plays an important dynamical role in the oscillation of the ENSO cycle by controlling the temperature of waters upwelled in the eastern equatorial Pacific (Jin 1997a,b), which in turn controls the coupling between the thermocline and SST there. The WWV anomaly is a convenient index for interpreting ENSO variability in terms of recharge oscillator paradigm (Jin 1997a,b; McPhaden 2004). According to this paradigm, a buildup (purge) of excess heat content (i.e., positive or negative WWV anomalies) along the equator is a prerequisite for the occurrence of El Niño (La Niña). The slowdown of the mean meridional overturning circulation in ABOT experiment delays the time it take to recharge (discharge) the equatorial region with excess heat, and causes a shift in the frequency of WWV variability. Figure 12 is same as Fig. 10b, but for the power spectra of the WWV anomalies. It is clearly shown that the primary peak of the WWV power spectrum for ABOT experiment in the last 60 years is also shifted to the 50th month (dashed line), while that for OT experiment remains unchanged (dotted line). This is quite consistent with the Nino-3 SST power spectra change in Fig. 10b.

The change in WWV tends to precede the change in Nino-3 SST by several months as found in observations (Meinen and McPhaden 2000; McPhaden 2004), and in our coupled model as well. Figure 13a shows the time series of the Nino-3 SST and WWV anomalies in ABOT control. These two variables have been band-filtered as in Fig. 5a. For clearness, only the data in the last 60 years are plotted. It is evident that positive WWV anomalies (or buildups of excess heat content) have almost preceded all El Niño events by about two seasons (Fig. 13a). The same relationship also exists between negative WWV anomalies (or purges of excess heat
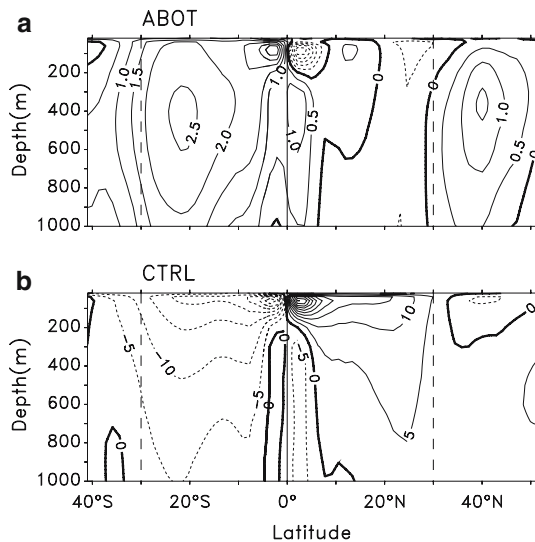

Fig. 11 Meridional overturning circulations in the upper Pacific for (**b**) the ABOT control and (**a**) the change in ABOT experiment averaged in the last 60 years. ABOT experiment shows more than 10% reduction in the mean meridional circulations in both hemispheres. The unit in (**a**) and (**b**) is Sv (1 Sv = 10^6 m³/s)
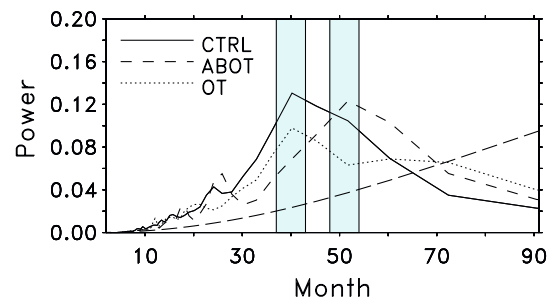

Fig. 12 Same as Fig. 10, but for the warm water volume (WWV) anomaly (5°N–5°S, 80°W–120°E above the 20°C isotherm) in the last 60 years. The WWV anomaly is obtained similarly as the Nino-3 SST anomaly

content) and La Niña events. The further analyses indicate that the peak correlation occurs with SST lagging WWV by 6 months in ABOT control (solid line in Fig. 13b) and 5 months in ABOT experiment (dashed line in Fig. 13b), with the maxima correlation coefficients of about 0.6 and 0.5, respectively. This is qualitatively consistent with the observational study by Meinen and McPhaden (2000), in which the maximum correlation ($r = 0.7$) occurs with SST lagging WWV by 7 months. These illustrate that the WWV is a reliable predictor of Nino-3 SST. The shift of ENSO frequency in ABOT experiment can be thus attributed to the shift of WWV frequency that resulted from the change in the strength of the mean meridional overturning circulation.

Here we further examine the relationship between the amplitude of WWV anomaly and the amplitude of Nino-3 SST anomaly in ABOT experiment, following the method of Meinen and McPhaden (2000). The seasonal averages of these two variables for the last 60 years are regressed against one another (Fig. 13c), in which the Nino-3 SST anomaly has been shifted backwards 5 months to maximize the cross correlation. It is apparent that in general, the larger WWV anomalies correspond to the larger Nino-3 SST anomalies. This is expectable because of the strong coupling between the thermocline and the SST, especially in the eastern equatorial Pacific Ocean.

Now it is understandable why the ENSO frequency in OT experiment keeps unchanged (dotted line in Fig. 10b). This is because the mean shallow meridional overturning circulation in OT experiment does not change, so does the frequency of the WWV variability. We also plot the power spectra of the Nino-3 SST in the first 20 years of the integrations of ABOT control, ABOT experiment, OT experiment and AB experiment (Fig. 10a), during which the Nino-3 SSTs in all experiments have the same primary peak located at the 40th month. This occurs because the subsurface ocean in ABOT in the first 20 years has not yet fully responded to the extratropical surface forcing. The AB alone does not appear to change the ENSO frequency, although it acts quickly. This is further confirmed by AB experiment (dotted–dashed line in Fig. 10a), in which only the AB conveys the extratropical forcing to the tropics, whereas the ocean is always in the climatological state.

5 Summaries and discussions

Idealized extratropical warming experiments in a coupled climate model are designed to anatomize the extratropical modulation of ENSO. Both the amplitude and frequency of ENSO are subject to change substantially in response to the extratropical forcing, in which the OT plays a more important role than the AB in changing the statistical properties of ENSO. The extratropical warming reduces the poleward SST contrast and immediately weakens the Hadley circulations in both
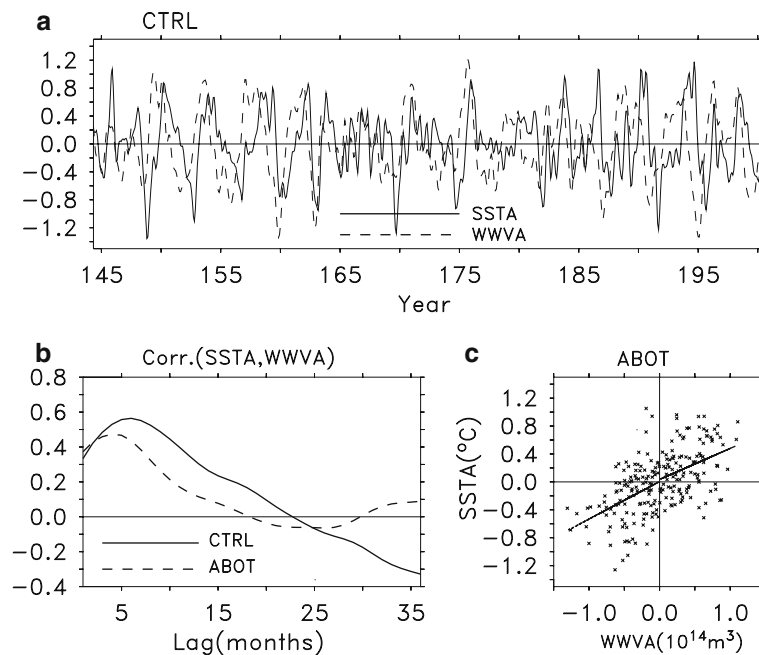

Fig. 13 a Time series of monthly anomalies of Nino-3 SST (*solid line*) and WWV (*dashed line*) in ABOT control. **b** Lagged cross correlations between Nino-3 SST and WWV in ABOT control (*solid line*) and experiment (*dashed line*). Correlations are for Nino3-SST lagging WWV. The peak correlations with WWV occur at the sixth month in ABOT control and the fifth month in ABOT experiment, with the values of about 0.6 and 0.5, respectively.

c Phase space of Nino-3 SST anomaly vs WWV anomaly for ABOT experiment. The SST time series has been shifted backward by 5 months to maximize the cross correlation between WWV and SST. *Lines* represent the linear regression of the SST on the WWV, separated into seasons with a negative WWV anomaly and those with a positive WWV anomaly

hemispheres. The latter further slows down the mean shallow meridional overturning circulation in the upper Pacific, resulting in a less equatorward cold water supply and a weaker equatorial upwelling. Consequently, the buildup (purge) of excess heat along the equator is slackened, which increases the time it take to recharge (discharge) the equatorial latitude, lengthens the period of the equatorial WWV variability and ultimately results in a longer ENSO period.

The extratropical warming can be conveyed to the equator by the mean subduction current, and cause a warmer equatorial thermocline that would be further enhanced by a less equatorward cold water supply resulted from the slowdown of the mean meridional overturning circulation. The stratification of equatorial thermocline can be, therefore, weakened. This, together with the relaxation of equatorial trade winds due to the weakened Hadley circulations, would stabilize the equatorial coupled system and result in a weaker ENSO variability. These dynamical mechanisms are summarized in Fig. 14, a flow chart illustrating briefly the causality of the extratropical modulation on ENSO.

The extratropical modulation on ENSO behavior is also justified by the observation studies that the ENSO regime shift in the 1970 s is closely linked to the regime shift in the North Pacific decadal oscillation (e.g., Zhang et al. 1998b), and a recent simplified coupled model study by Sun et al. (2004), who identified an increase in ENSO amplitude by an enhanced subtropical cooling. The stronger subtropical cooling reduces the temperature of the water feeding the equatorial undercurrent through the OT. The resulting colder equatorial upwelling water tends to increase the equatorial zonal SST contrast. The ENSO strengthens in response to this destabilizing forcing. Note that the atmosphere component in Sun et al. (2004) includes only the zonal wind that simply coupled to the zonal SST contrast. As a

result, the Bjerknes positive feedback works very well. This is different from our model in which the tropical wind change is nonlocally determined by Hadley circulation change.

This work suggests a nonlocal mechanism for the change of ENSO statistics, based on the assumption that the tropical background state and thus the stability of the tropical coupled ocean–atmosphere system could be remotely determined by the extratropics. Here we highlight the dominant role of the OT in ENSO change in an equilibrium system. In particular, the change in ENSO frequency appears to have to invoke the change in the mean oceanic meridional overturning circulation. The AB alone seems to have no contribution to ENSO frequency change. It is likely that local nonlinearity within the tropics could result in the ENSO change (e.g., Timmermann and Jin 2002). This is beyond the scope of this paper.

This work can be also understood as a study of ENSO sensitivity to an idealized global warming. Our experiments are designed to study the *equilibrium* response of the tropical ENSO to a sudden onset of extratropical warming (Liu 1998). The global upper oceans in our experiments have reached quasi-equilibrium after 200 years integration, which finally determine the tropical thermocline structure and the stability of the tropical coupled system. In a climate forced by a transient CO_2, the upper ocean may not have yet reached *equilibrium*. The tropical climate at large may be thus determined by the atmospheric processes, which could result in a different ENSO response. It would be very interesting to examine the *equilibrium* response of ENSO behavior to a sudden increased CO_2.

Currently, instead of focusing on global warming, we have performed a global "cooling" experiment using the same model, in which the solar constant is suddenly reduced by 8 W/m^2. This simulation has been integrated

Fig. 14 Flow chart illustrating the causality of the extratropical modulation on ENSO
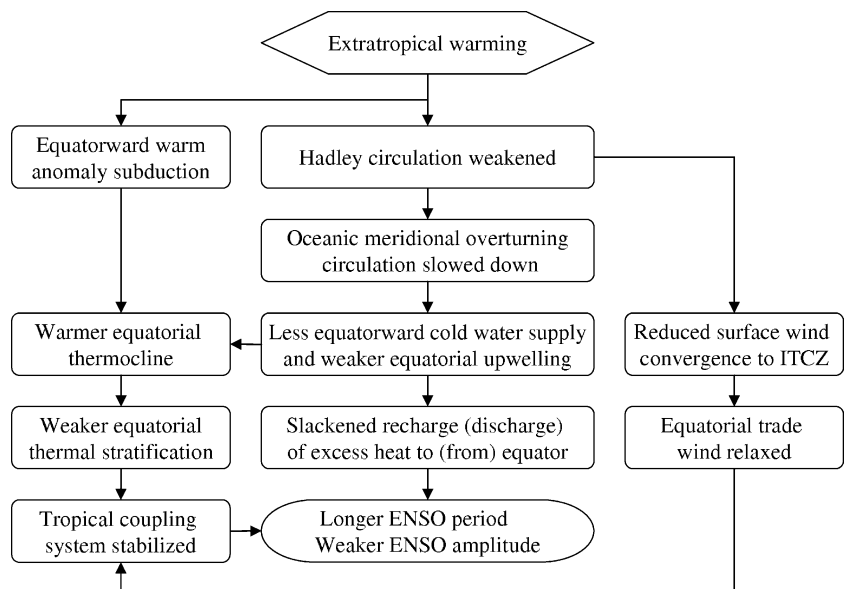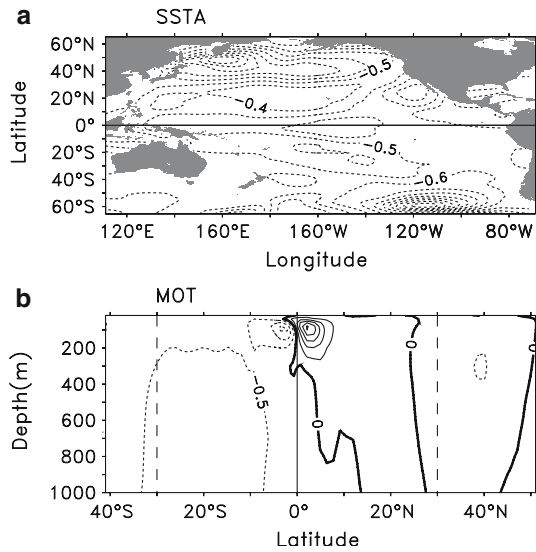
Fig. 15 SST change (**a**) and the mean meridional overturning circulation change (**b**) in the upper Pacific averaged in the last 50 years of the SOLAR run (with solar constant reduced by 8 W/m^2)

for 130 years and the last 50 years data are analyzed. The quasi-equilibrium response of the Pacific SST (Fig. 15a) shows that there are three SST cooling maxima located at 35–60° in both hemispheres (−0.9°C for the North Hemisphere and −1.2°C for the South Hemisphere) and the central-east equatorial Pacific (−0.6°C), respectively. This SST pattern is nearly antisymmetric to that in PC experiment of ABOT (Yang and Liu 2005). In response to the enhanced poleward SST contrast, the Hadley circulations in both hemispheres as well as the equatorial trade winds are intensified (figure not shown), which further results in a speedup of the
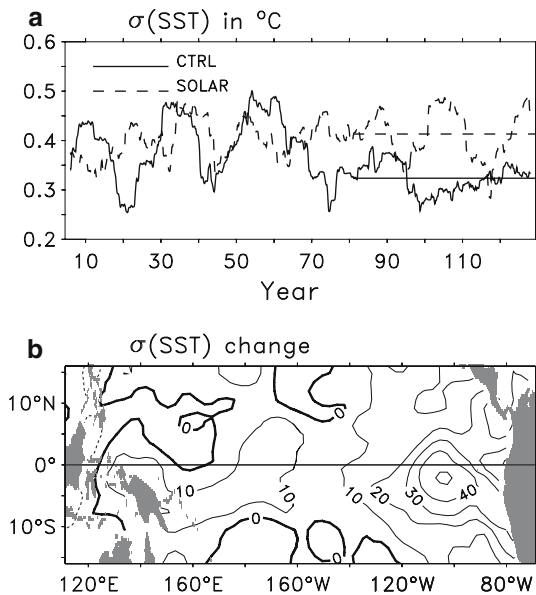
mean shallow meridional overturning circulation in the upper Pacific. Figure 15b indicates that the strength of overturning circulations in both hemispheres, especially the local equatorial cells in the upper 200 m, is nearly symmetrically increased by about 10%. These destabilize the tropical coupled system due to an increased cold water supply from the extratropics at depth and a stronger equatorial upwelling. The Nino-3 SST amplitude is increased by as much as 28% (Fig. 16a). The tropical SST variability is increased by nearly 30% in the eastern tropical Pacific (Fig. 16b). Our studies suggest that the responses of ENSO to a changing climate are complex due to the complexity of the ocean–atmosphere coupled system.

References

Alexander MA, Blade I, Newman M, Lanzante JR, Lau N-C, Scott JD (2002) The atmospheric bridge: the influence of ENSO teleconnections on air–sea interaction over the global oceans. J Clim 15:2205–2231

Barnett T, Pierce DW, Latif M, Dommenget D, Saravana R (1999) Interdecadal interactions between the tropics and the midlatitudes in the Pacific basin. Geophys Res Lett 26:615–618

Cole J (2001) A slow dance for El Niño. Science 291:1496–1497

Collins M (2000a) Understanding uncertainties in the response of ENSO to greenhouse warming. Geophys Res Lett 27:3509–3513

Collins M (2000b) The El-Niño–Southern Oscillation in the second Hadley Centre coupled model and its response to greenhouse warming. J Clim 13:1299–1312

Enfield DB, Mayer DA (1997) Tropical Atlantic sea surface temperature variability and its relation to El Niño–Southern Oscillation. J Geophys Res 102:929–945

Fedorov AV, Philander SG (2000) Is El Niño changing? Science 288:1997–2002

Fedorov AV, Philander SG (2001) A stability analysis of Tropical ocean–atmosphere interaction: bridging measurements and theory for El Niño. J Clim 14:3086–3101

Gu D, Philander SGH (1997) Interdecadal climate fluctuations that depend on exchanges between the tropics and extratropics. Science 275:805–807

Hoerling MP, Hurrell JW, Xu T (2001) Tropical origins for recent North Atlantic climate change. Science 292:90–92

Jacob (1997) Low frequency variability in a simulated atmosphere ocean system. Ph.D. thesis, University of Wisconsin–Madison, 155p

Jin F-F (1997a) An equatorial ocean recharge paradigm for ENSO. Part I: conceptual model. J Atmos Sci 54:811–829

Jin F-F (1997b) An equatorial ocean recharge paradigm for ENSO. Part II: a stripped-down coupled model. J Atmos Sci 54:830–847

Kleeman R, McCreary JP, Klinger BA (1999) A mechanism for generating ENSO decadal variability. Geophys Res Lett 26:1743–1746

Fig. 16 Same as Fig. 9, but for the SOLAR run

Knutson TR, Manabe S, Gu D (1997) Simulated ENSO in a global coupled ocean model: multidecadal amplitude modulation and CO_2 sensitivity. J Clim 10:138–161

Lau N-C (1997) Interactions between global SST anomalies and the midlatitude atmospheric circulation. Bull Am Meteorol Soc 78:21–33

Liu Z (1998) The role of ocean in the response of tropical climatology to global warming: the west–east SST contrast. J Clim 11:864–875

Liu Z, Wu L (2000) Tropical Atlantic Oscillation in a coupled GCM. Atmos Sci Lett 1:26–36

Liu Z, Yang H (2003) Extratropical control of tropical climate, the atmospheric bridge and oceanic tunnel. Geophys Res Lett 30(5) (doi: 10.1029/2002GL016492)

Liu Z, Philander SGH, Pacanowski R (1994) A GCM study of tropical–subtropical upper ocean mass exchange. J Phys Oceanogr 24:2606–2623

Liu Z, Kutzbach J, Wu L (2000) Modeling climate shift of El Niño variability in the Holocene. Geophys Res Lett 27:2265–2268

Liu Z, Wu L, Gallimore R, Jacob R (2002) Search for the origins of Pacific decadal climate variability. Geophys Res Lett 29(10) (doi: 10.1029/2001GL013735)

Lu J, Greatbatch RJ, Peterson KA (2004) Trend in northern hemisphere winter atmospheric circulation during the last half of the 20th century. J Clim 17:3745–3760

McCreary J, Lu P (1994) On the interaction between the subtropical and the equatorial oceans: the subtropical cell. J Phys Oceanogr 24:466–497

McPhaden MJ (2004) Evolution of the 2002/03 El Niño. Bull Am Meteorol Soc 85:677–695

Meehl GA, Branstator GW, Washington WM (1993) Tropical Pacific interannual variability and CO_2 climate change. J Clim 6:42–63

Meinen CS, McPhaden MJ (2000) Observations of warm water volume changes in the equatorial Pacific and their relationship to El Niño and La Niña. J Clim 13:3551–3559

Pierce DW, Barnett TP, Latif M (2000) Connections between the Pacific Ocean Tropics and midlatitudes on decadal timescales. J Clim 13:1173–1194

Rosenthal Y, Broccoli AJ (2004) In search of Paleo-ENSO. Science 304:219–221

Sun D-Z, Zhang T, Shin S-I (2004) The effect of subtropical cooling on the amplitude of ENSO: a numerical study. J Clim 17:3786–3798

Tett S (1995) Simulations of El Niño–Southern Oscillation-like variability in a global AOGCM and its response to CO_2 increase. J Clim 8:1473–1502

Timmermann A (2001) Changes of ENSO stability due to greenhouse warming. Geophys Res Lett 28(10):2061–2064 (10.1029/2001GL012879)

Timmermann A, Jin F-F (2002) A nonlinear mechanism for decadal El Niño amplitude changes. Geophys Res Lett 29(1) (10.1029/2001GL013369)

Timmermann A, Latif M, Bacher A, Oberhuber J, Roeckner E (1999) Increased El Niño frequency in a climate model forced by future greenhouse warming. Nature 398:694–696

Tudhope AW, et al (2001) Variability in the El Niño–Southern Oscillation through a glacial–interglacial cycle. Science 291:1511–1517

Wang C (2002) Atlantic climate variability and its associated atmospheric circulation cells. J Clim 15:1516–1536

Wang C, Weisberg RH (1998) Climate variability of the coupled tropical–extratropical ocean–atmosphere system. Geophys Res Lett 25(21):3979–3982

Weaver AJ (1999) Extratropical subduction and decadal modulation of El Niño. Geophys Res Lett 26:743–746

Wu L, Liu Z, Gallimore R, Jacob R, Lee D, Zhong Y (2003) Pacific decadal variability: the Tropical Pacific mode and the North Pacific mode. J Clim 16:1101–1120

Yang H, Liu Z (2005) Tropical–extratropical climate interaction as revealed in idealized coupled climate model experiments. Clim Dyn (DOI 10.1007/s00382-005-0021-8)

Yu L, Rienecker MM (1999) Mechanisms for the Indian Ocean warming during 1997–1998 El Niño. Geophys Res Lett 26:735–738

Zelle H, Appeldoorn G, Burgers G, Oldenborgh GV (2004) The relationship between sea surface temperature and thermocline depth in the eastern equatorial Pacific. J Phys Oceanogr 34:643–655

Zhang Y, Wallace JM (1996) Is climate variability over the North Pacific a linear response to ENSO? J Clim 11:1468–1478

Zhang X, Sheng J, Shabbar A (1998a) Modes of interannual and interdecadal variability of Pacific SST. J Clim 11:2556–2569

Zhang RH, Rothstein LM, Busalacchi AJ (1998b) Origin of warming and El Niño change on decadal scales in the tropical Pacific Ocean. Nature 391:879–883